International Journal of Heat and Mass Transfer 65 (2013) 627–634

Contents lists available at SciVerse ScienceDirect

International Journal of Heat and Mass Transfer

journal homepage: www.elsevier.com/locate/ijhmt

Gas dispersion of oscillatory flow in expanding and contracting multi-branching airways

Toshihiro Sera [a,b,*], Hideo Yokota [b], Ryutaro Himeno [c], Gaku Tanaka [d]

[a] The Center for Advanced Medical Engineering and Informatics, Osaka University, 2-15, Yamadaoka, Suita, Osaka 565-0871, Japan
[b] Bio-research Infrastructure Construction Team, RIKEN, 2-1, Hirosawa, Wako, Saitama 351-0198, Japan
[c] Advanced Center for Computing and Communication, RIKEN, 2-1, Hirosawa, Wako, Saitama 351-0198, Japan
[d] Department of Mechanical Engineering, Graduate School of Engineering, Chiba University, 1-33 Yayoi-cho, Inage-ku, Chiba 263-8522, Japan

ARTICLE INFO

Article history:
Received 18 March 2013
Received in revised form 21 June 2013
Accepted 21 June 2013
Available online 17 July 2013

Keywords:
Respiratory system
Gas dispersion
Airway motion
Steady streaming
Oscillatory flow

ABSTRACT

Mass transport phenomena in airways, including dispersion, may be influenced by the complicated three-dimensional (3D) branching geometry, which undergoes expansion and contraction during the respiratory cycle. In this study, we investigated the effects of this expansion and contraction on gas dispersion in multi-branching airways using computational fluid dynamics. A 3D multi-branching airway model was constructed based on mammalian computed tomography images, with diameters ranging from 1.25 mm in the parent tube to 0.35 mm in the daughter tube. We examined the dispersion of oxygen in the airway when subject to oscillatory flow while the airway expanded and contracted sinusoidally with time. After several respiratory cycles, the oxygen fraction was higher in the airway-motion model than in the rigid model, and it increased as the volume expansion factor increased. Furthermore, the oxygen fraction increased as the breathing frequency was increased for the airway model undergoing wall motion. Transport simulation of passive tracer particles showed that, although the particles were dispersed around the initial position in the rigid model, many particles were anchored around the carina and dispersed widely in the airway-motion model. These results indicate that steady streaming and unsteady flow behavior due to airway branches and expanding and contracting motion may enhance gas dispersion in multi-branching airways.

1. Introduction

The mammalian airway tree consists of a system of multiple-branched tubes originating within the trachea, dividing by asymmetrical dichotomy into progressively shorter and smaller diameter bronchi and then bronchioles as far as the terminal bronchioles. As the airway progresses from the trachea to the terminal bronchioles, the airway diameter decreases exponentially, but the total cross-sectional area of two daughter branches is usually greater than that of the parent. In particular, within the peripheral airways, the cross-sectional area increases rapidly with successive airway branching. Consequently, the flow velocity decreases. Additionally, the flow inertia and unsteadiness are usually negligible. The flow characteristics and mass transport mechanisms change significantly with each branching generation [1–3].

Mass transport in the respiratory tract is achieved through a combination of convection and diffusion. Various mechanisms have been proposed to explain convective mixing in the lung, including axial streaming, augmented dispersion, and steady streaming. Briefly, axial streaming consists of longitudinal transport with axial velocity; augmented dispersion mainly results from turbulence and secondary flow [4] in main conducting airways, and Taylor dispersion [5] in small airways; steady streaming is due to the difference in the velocity profile between inspiration and expiration [6,7]. In main conducting airways, the secondary vortex in curved tubes enhances transport by mixing in the cross-section [4]. In small airways, laminar Taylor dispersion is corresponding to a situation where the evolution of radial mass fraction gradients by axial streaming is in balance with their relaxation by radial diffusion [8]. Fresconi and Parasad [9] experimentally investigated the dispersion mechanisms that occur during steady-state flow and reported that simple axial streaming, rather than augmented dispersion, is the dominant steady-state convective dispersion in symmetric airways. They also suggested that not only the different transport structures during inspiration and expiration, but also the branching nature of the airways, contributed to steady streaming in the lung.

During ventilation of the lung, both the bronchial tree and alveolar regions of the lung expand and contract, even though the

* Corresponding author at: The Center for Advanced Medical Engineering and Informatics, Osaka University, 2-15, Yamadaoka, Suita, Osaka 565-0871, Japan. Tel.: +81 6 6850 6183; fax: +81 6 6850 6212.
E-mail address: sera@me.es.osaka-u.ac.jp (T. Sera).

0017-9310/$ - see front matter © 2013 Elsevier Ltd. All rights reserved.
http://dx.doi.org/10.1016/j.ijheatmasstransfer.2013.06.051

deformation is larger in alveolar regions [10,11]. The larger airways of the trachea and main bronchus are supported by both cartilaginous rings and smooth muscle. However, as the airways become smaller, the amount of cartilage decreases and the amount of smooth muscle increases. The walls of the peripheral regions are thinner and more flexible than those of the conducting airways, and expand and contract considerably during breathing. In comparison with 0 cmH_2O of lung pressure, the diameter increment of conducting airways and small airways are approximately 50% and 150% at 20 cmH_2O of lung pressure, respectively [10]. Tsuda et al. [12] and Henry et al. [13] calculated the alveolar duct flow using a simple pulmonary acinar model consisting of a straight tube with a single sphere, and found acinar flow exhibiting multiple saddle points, characteristic of chaotic flow, resulting in substantial flow irreversibility. Tanaka el al. [14] investigated the kinematic irreversibility of flow in expansion and contraction of true-geometry small airways using numerical simulation of the oscillatory flow in a 3D small airway model, with diameters in the range of 55–360 μm.

In peripheral airways, internal transport phenomena are characterized by low-Reynolds (*Re*)-number flow [14]. The conventional theory of gas mixing asserts that the *Re* is approximately zero and that gas transport is dominated by simple diffusion [3]. However, important fluid dynamics phenomena in the peripheral airways, such as gas dispersion, are influenced by the complicated three-dimensional (3D) branching geometry, which expands and contracts during breathing.

In this study, we investigated gas dispersion resulting from the kinematic irreversibility of flow during expansion and contraction of the airways. The airway geometry was reconstructed from synchrotron-based computed tomography (CT) images of rat lungs [10]. Using both a rigid model and an expansion–contraction model in which the moving boundary conditions induce airway expansion and contraction with the volume changing sinusoidally with time [12,14–20], we assessed dispersion of oxygen into air-filled airways under variable flow conditions. We hypothesise that gas dispersion is enhanced by expanding and contracting breathing motion of multi-branching airways.

2. Numerical methods

We reconstructed the multi-branching airway geometry using synchrotron-based CT images of rat lungs, and assumed that O_2 at the parent inlet diffused into the air-filled airway during breathing cycles in which the volume of the lung changed sinusoidally with time.

2.1. Multi-branching airway model

Fig. 1 shows CT cross-sectional images of the rat lung after segmentation. The isotropic voxel size was 48 μm, and the resolution was $1000 \times 1000 \times 280$. We identified the cross-sections of the small airways using a threshold-based, 3D, region-growing algorithm using the commercially available software package Amira (Visage Imaging, Germany). The threshold value was preselected, leading to an optical segmentation result. In general, the image intensity of air is less than that of lung tissue. Starting from a seeding voxel defined by the user, the algorithm accumulates all the voxels with an intensity below the threshold. We measured histograms of the pixel intensity around the target airway and defined the threshold at the highest gradient of the histogram; interactive correction of this threshold value was carried out.

Fig. 2 shows the segmented multi-branching airway model. To avoid any influence of the boundary conditions on the computer simulation, each branch was artificially lengthened with a straight

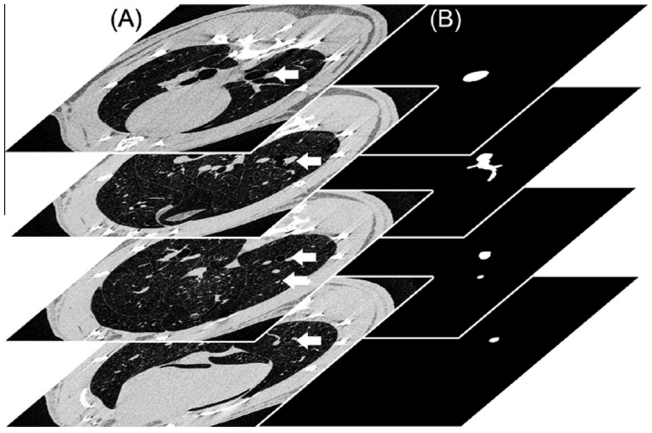

Fig. 1. CT images ((A) original CT images, (B) segmented CT images) of a live rat lung. Arrows in A indicate the segmented airways.

tube in the direction of the skeleton calculated using a 3D thinning algorithm. This algorithm performs a Euclidean distance (the distance from the background) transformation and, as the voxels are deleted in sequence, repeatedly checks that the Euclidean distance is small. Finally, the middle line is located corresponding to the branching point of the airway network without altering the topology. The dimensions of the simulation domain were $8.9 \times 12 \times 20$ mm. The model had multiple branches from one parent tube with a diameter of 1.25 mm to 41 daughter tubes with minimum diameters of 0.35 mm. The parent tube was connected to the central airways, and the daughter tubes to the distal airways.

2.2. Mesh generation

The computational mesh was generated using ICEM CFD (ANSYS, Inc.). We created an irregular mesh with tetrahedral elements for the core. Three subsurface layers with prism volume elements were inserted along the walls to increase the accuracy of the simulation where the velocity gradients were largest. The mesh consisted of 2 157 000 elements.

The dependency of the solution on the mesh was examined by solving the flow fields and gas dispersions for various mesh configurations ranging from 193 000 to 5 732 000 elements. Velocity profiles, gas dispersion, and particle dispersion were compared in several sections for all mesh configurations. The differences in the maximum velocity and averaged oxygen fractions in the final model were less than 0.5% when the mesh density was increased beyond 2 157 000 elements.

2.3. Numerical methods

Assuming isothermal, laminar, incompressible airflow, the governing equations were as follows, assuming conservation of mass, momentum, and advection–diffusion:

$$\nabla \cdot u = 0 \tag{1}$$

$$\frac{\partial u}{\partial t} + (u \cdot \nabla)u = -\frac{1}{\rho}\nabla p + v\nabla^2 u \tag{2}$$

$$\frac{\partial C}{\partial t} + u\nabla C = D\nabla^2 C \tag{3}$$

where u is the velocity vector of the fluid, p is the pressure, v is the kinematic viscosity ($=1.461 \times 10^{-5}$ m^2/s), ρ is the density ($=1.225$ kg/m^3), C is the gas concentration, and D is the diffusion coefficient for O_2 in air, which was taken to be 0.25 cm^2/s [8]. To